Available online at www.sciencedirect.com

ScienceDirect

Procedia Structural Integrity 25 (2020) 101–111

Structural Integrity Procedia

www.elsevier.com/locate/procedia

1st Virtual Conference on Structural Integrity - VCSI1

More on variance of fatigue damage in non-Gaussian random loadings – effect of skewness and kurtosis

Julian Marcell Enzveiler Marques*, Denis Benasciutti

Department of Engineering, University of Ferrara, via Saragat 1, 44122, Ferrara, Italy

Abstract

This work investigates the variance of fatigue damage in stationary random loadings with non-Gaussian probability distribution and narrow-band power spectral density. It presents an approach exploiting a non-linear time-invariant transformation that links Gaussian and non-Gaussian domains and that is calibrated on the skewness and kurtosis values of the non-Gaussian process. The transformation allows determining the joint probability distribution of two peaks and the cycle amplitude distribution in the non-Gaussian process, from which the variance of damage is calculated. Monte Carlo numerical simulations are finally discussed to demonstrate the correctness of the proposed model and to investigate the sensitivity of the damage variance to several parameters (S-N inverse slope, skewness and kurtosis of non-Gaussian loading).

Keywords: Variance of fatigue damage; non-Gaussian; kurtosis; skewness; random loadings

1. Introduction

There are many engineering applications in which mechanical components are subjected to loadings inherently random, that is loadings with a random nature. Examples are the loads from road irregularity, wind or sea waves. Assessing the component structural durability usually requires that loading sample records be processed by counting

* Corresponding author. Tel.: +39-0532-974104; fax.: +39-0532-974870
E-mail address: nzvjnm@unife.it

10.1016/j.prostr.2020.04.014

methods and damage accumulation rules (e.g. rainflow counting and Palmgren-Miner rule) so to compute a fatigue damage value from which the component service life is estimated.

Nomenclature

$\hat{C}_{\mathrm{D}}$	sample coefficient of variation	$(x_{\mathrm{p}}, x_{\mathrm{v}})$, $(z_{\mathrm{p}}, z_{\mathrm{v}})$	peak and valley (Gaussian, non-Gaussian)
C_{D}	coefficient of variation of fatigue damage	$x(t)$, $z(t)$	Gaussian and non-Gaussian time-history
d	fatigue damage of a half-cycle	$X(t)$, $Z(t)$	Gaussian and non-Gaussian process
$\overline{D}$	sample mean of fatigue damage	γ_3, γ_4	skewness, kurtosis
$D(T)$	fatigue damage in time period T	λ_{m}	m-th spectral moment
$f_{\mathrm{a}}(s)$	probability distribution of stress amplitudes	μ_{X}, μ_{Z}	mean value of $X(t)$ and $Z(t)$
$f_{\mathrm{P_0,P_1}}(-)$	joint probability density function of two peaks	ν_0^+	rate of mean value upcrossings
$G(-)$, $g(-)$	direct and inverse transformation	$\rho_{\mathrm{X}}(\tau)$, $\rho_{\mathrm{Z}}(\tau)$	autocorrelation coefficient of $X(t)$ and $Z(t)$
k, A	material constants of the S-N curve	$\hat{\sigma}_{\mathrm{D}}^2$	sample variance of fatigue damage
$n(T)$	number of counted cycles in T	σ_{D}^2	variance of fatigue damage
$R_{\mathrm{X}}(\tau)$	correlation function of $X(t)$	σ_{X}^2, σ_{Z}^2	variance of $X(t)$ and $Z(t)$
s	stress amplitude of a half-cycle	τ	time lag
$S_{\mathrm{X}}(f)$	Power Spectral Density of $X(t)$	${}^{\mathrm{G}}y$, ${}^{\mathrm{nG}}y$	(pre-superscript) Gaussian, non-Gaussian

Sample records from random loadings do have fatigue cycles that vary randomly both in their number as well as in their amplitudes and mean values. Fatigue cycles, and the damage computed therefrom, are thus random variables. This means that, for example, different damage values would result when analyzing distinct loading records, even if measured under virtually identical conditions.

It often happens, though, that only few (perhaps only one) sample records of limited time length are available in practice. This small sample may give an incomplete picture of the cycle distribution characterizing the random loading. The computed damage may thus be a biased estimate of the "true" (or average) damage that would result by processing a much larger set of loading sample records, or ones with a much longer time duration. In other words, few damage values may have so large levels of statistical variability to make any fatigue life estimation rather uncertain (which, in turn, requires high safety factors to be introduced). Estimating the statistical variability (variance) of the damage is thus as equally important as estimating the "average" damage value.

Over the last decades, several theoretical solutions were developed (e.g. Low, Mark and Crandall, Bendat) for estimating the variance of damage in a stationary random loading that is Gaussian and has a narrow-band frequency spectrum. Gaussian means that the load values follow a normal distribution; narrow-band means that the spectrum is concentrated around a well-defined frequency, as it happens in structures vibrating at their first resonance.

The previous theoretical solutions do not apply, however, to loadings that are not Gaussian. This class of loadings is encountered, for instance, if the loading is itself non-Gaussian (e.g. certain types of wind or wave loads) or if a structure has a nonlinearity that transforms a Gaussian input into a non-Gaussian stress response (Benasciutti and Tovo (2018)).

It should be noted that the non-Gaussian case is of particular relevance in structural durability. Indeed, a non-Gaussian loading with kurtosis>3 takes on values larger than a corresponding Gaussian one with same variance, so its damage will be larger–and its variance different–from what predicted by Gaussian models.

This premise emphasizes the importance to extend the current solutions of the damage variance from the Gaussian to the non-Gaussian case, which is indeed the main purpose of the present work. A "transformed model", which links the Gaussian and non-Gaussian domains, is used by the approach here proposed to extend the Low's solution to the case of a non-Gaussian narrow-band loading. The transformed model forms the basis from which the joint probability distribution of two peaks in the non-Gaussian process is derived. Through a numerical solution, the proposed method arrives at estimating the variance for any combination of skewness and kurtosis of practical interest.

A Monte Carlo study is finally carried out, with two main purposes. The first is to verify the correctness of the proposed solution. The second is to investigate how much the variance of damage depends on the values of skewness and kurtosis of the non-Gaussian process, as well as on the inverse slope of S-N curve.

2. Theoretical background

2.1. Random process and Power Spectral Density (PSD)

Let $X(t)$ be a stationary Gaussian random process. It represents an infinite collection (ensemble) of time histories of unlimited duration, $x_{\mathrm{i}}(t)$, $-\infty < t < \infty$. The process $X(t)$ has mean value μ_{X} and autocorrelation function $R_{\mathrm{X}}(\tau) = E[X(t)X(t+\tau)]$. An autocorrelation coefficient, $\rho_{\mathrm{X}}(\tau) = R_{\mathrm{X}}(\tau)/\sigma_{\mathrm{X}}^2$, (with $-1 \leq \rho_{\mathrm{X}}(\tau) \leq 1$) will also be used in the following. The Fourier transform of $R_{\mathrm{X}}(\tau)$ defines the one-sided Power Spectral Density (PSD) $S_{\mathrm{X}}(f)$ of the random process. The power spectrum has spectral moments:

$$\lambda_m = \int_0^\infty f^m \, S_X(f) \, df, \quad m = 0,1,2 \ldots \tag{1}$$

The variance of $X(t)$ is $\lambda_0 = \sigma_{\mathrm{X}}^2$ and the frequency of upward crossings of the mean value is ${}^{\mathrm{G}}\nu_0^+ = \sqrt{\lambda_2/\lambda_0}$ (the pre-superscript specifies the Gaussian process).

Let $Z(t)$ be a non-Gaussian random process, with mean μ_{Z} and upcrossing rate ${}^{\mathrm{nG}}\nu_0^+$ (the pre-superscript stands for non-Gaussian). The values of a non-Gaussian process do not follow a Gaussian probability distribution. The degree of deviation from the Gaussian distribution is summarized by the skewness and kurtosis parameters:

$$\gamma_3 = \frac{E[(Z-\mu_Z)^3]}{\sigma_Z^3} \; skewness; \qquad \gamma_4 = \frac{E[(Z-\mu_Z)^4]}{\sigma_Z^4} \; kurtosis \tag{2}$$

where symbol $E[-]$ means "expected value". The skewness quantifies the degree of asymmetry of the non-Gaussian distribution. The kurtosis quantifies the contribution of the tails of the distribution: values away from the mean can be either higher ($\gamma_4 > 3$, leptokurtic case) or lower ($\gamma_4 < 3$, platykurtic case) than the values from a Gaussian distribution, for which $\gamma_3 = 0$ and $\gamma_4 = 3$.

3. Fatigue damage: expected value and variance

Let $x(t)$, $0 < t < T$, be a time history of time duration T. Under the Palmgren-Miner hypothesis, the fatigue damage $D(T)$ is calculated as the sum of damage values of $n(T)$ individual half-cycles counted in T:

$$D(T) = \sum_{i=1}^{n(T)} d_i = \sum_{i=1}^{n(T)} \frac{s_i^k}{2A} \tag{3}$$

where s_{i} is the stress amplitude of the *i*-th half-cycle; k and A are material constants defining the S–N curve as $s^{\mathrm{k}}N = A$. Damage $D(T)$ depends on the particular set of stress amplitudes s_{i} counted in $x(t)$. It is a function of the particular $x(t)$ from which it is computed, as well as of the time duration T. For example, the damage would take a different value if $x(t)$ were longer, or if the damage were computed from another realization of the random process.

Taking the expectation of Eq. (1) gives the expected damage value:

$$E[D(T)] = E[n(T)] \frac{E[s^k]}{2A} \tag{4}$$

It represents the limiting case in which the damage is computed from the whole ensemble of realizations, or from an ergodic time history of infinite time length. The quantity $E[n(T)]$ is the expected number of cycles counted in T, whereas the term $E[d] = E[s^{\mathrm{k}}]/2A$ represents the expected damage per half-cycle, calculated from the probability distribution of stress amplitudes $f_{\mathrm{a}}(s)$ as (Benasciutti and Tovo (2005)):

$$E[d] = \frac{1}{2A}\int_0^\infty s^k f_a(s)\, ds \tag{5}$$

In a narrow-band Gaussian process, $f_{\mathrm{a}}(s)$ is a Rayleigh distribution and the damage per half-cycle becomes:

$$^{G}E[d] = \frac{1}{2A}\left(\sqrt{2\lambda_0}\right)^k \Gamma\left(1+\frac{k}{2}\right) \tag{6}$$

where $\Gamma(-)$ is the gamma function. Superscript specifies the Gaussian case. Furthermore, in a narrow-band process the expected number of half-cycles is twice the number of mean value upward crossings, $E[n(T)] = 2\nu_0^+ T$.

The variance of $D(T)$ is obtained by simply taking the variance of Eq. (3) (Mark (1961)):

$$\sigma_D^2 = Var\left[\sum_{i=1}^{n(T)} d_i\right] = E\left[\sum_{i=1}^{n(T)}\sum_{j=1}^{n(T)} d_i d_j\right] - \left(E\left[\sum_{i=1}^{n(T)} d_i\right]\right)^2 \tag{7}$$

The second equality follows from the definition of the variance of a random variable $Var(y) = E[y^2] - (E[y])^2$.

A deterministic number of half-cycles $n(T)$ can be assumed if peaks and valley that define every half-cycle are mutually independent and identically distributed. The variance then becomes:

$$\sigma_D^2 = \sum_{i=1}^{n}\sum_{j=1}^{n} E\left[d_i d_j\right] - \left(\sum_{i=1}^{n} E[d_i]\right)^2 \tag{8}$$

As the random process $X(t)$ is stationary, the discrete process d_{i} can be assumed to be stationary as well, so that $E[d_0] = E[d_1] = \cdots = E[d_{\mathrm{n}-1}]$ and $E\left[d_{\mathrm{i}} d_{\mathrm{j}}\right] = E[d_0 d_{\mathrm{l}}]$, $l = j - i$. Accordingly, the previous equation turns into:

$$\sigma_D^2 = n(E[d_0^2] - E[d_0]^2) + 2\sum_{l=1}^{n-1}(n-l)(E[d_0 d_l] - E[d_0]^2) \tag{9}$$

The term $(n-l)E[d_0 d_{\mathrm{l}}]$ characterizes the autocorrelation function $R_{\mathrm{d_0,d_l}}(l)$ of the half-cycle damage, where l is the "time lag" that takes on integer values from 1 to $n-1$.

Now consider two peaks, P_0 and P_{l}, separated by a time difference $\tau = l/(2\nu_0^+)$. Following Low (2012), throughout the text the term ''peaks'' is used in a broad sense to mean also valleys. It should be noted that, in a narrow-band process, the stress amplitude is equal to the peak value, $s_{\mathrm{l}} = P_{\mathrm{l}}$. Therefore, the damage per cycle d_{l} is proportional to $P_{\mathrm{l}}^{\mathrm{k}}$. Accordingly, the product $E[d_0 d_{\mathrm{l}}]$ can be computed from the joint probability density function (JPDF) of two peaks, $f_{\mathrm{P_0,P_l}}(x_{\mathrm{p}}, x_{\mathrm{v}})$ as:

$$E[d_0 d_l] = \frac{1}{4A^2}\iint_{-\infty}^{\infty} x_p^k x_v^k\, f_{P_0,P_l}(x_p, x_v)\, dx_p\, dx_v \tag{10}$$

This equation makes apparent that $E[d_0 d_{\mathrm{l}}]$ depends upon the JPDF $f_{\mathrm{P_0,P_l}}(x_{\mathrm{p}}, x_{\mathrm{v}})$, which thus plays a fundamental role to compute the variance by Eq. (9). A general closed-form expression for $f_{\mathrm{P_0,P_l}}(x_{\mathrm{p}}, x_{\mathrm{v}})$ is not available, unless some simplifying hypothesis are introduced, as proposed in several approaches (Low, Mark and Crandall, Bendat). A survey can be found in Enzveiler Marques et al. (2019). In the next paragraph, only a brief account of Low's approach for Gaussian processes is presented, as it constitutes the basis from which to develop the method for non-Gaussian processes.

4. Variance of damage: Gaussian case (Low's method)

This method is applicable to Gaussian narrow-band processes with any spectral density shape. For this process, the JPDF of two peaks has been derived by Rice (1944):

$$ {}^{G}f_{P_{0},P_{l}}(x_p, x_v) = \frac{x_p x_v}{1-\rho_X^2} I_0\left(\frac{x_p x_v\, \rho_X}{1-\rho_X^2}\right) e^{\frac{x_p^2+x_v^2}{-2(1-\rho_X^2)}} \tag{11} $$

where $I_0(-)$ is the modified Bessel function of the first kind with order zero, and $\rho_{\mathrm{X}} = \rho_{\mathrm{X}}(l)$ is the autocorrelation coefficient computed at the lag l. By invoking Eq. (9), the variance is:

$$ {}^{G}\sigma_D^2 = n\left({}^{G}E[d_0^2] - {}^{G}E[d_0]^2\right) + 2\sum_{l=1}^{n-1}(n-l)\left({}^{G}E[d_0^2] - {}^{G}E[d_0]^2\right) {}^{G}\rho_{d_0,d_l} \tag{12} $$

The quantity ${}^{\mathrm{G}}\rho_{\mathrm{d_0,d_l}}$ is the damage correlation coefficient. In Low (2012) it is computed by means of the joint distribution in Eq. (11) and approximated by a quadratic interpolation function of ρ_{X}^2 as ${}^{\mathrm{G}}\rho_{\mathrm{d_0,d_l}} = \alpha_{\mathrm{k}}\rho_{\mathrm{X}}^2 + \beta_{\mathrm{k}}\rho_{\mathrm{X}}^4$, where α_{k} and β_{k} are best-fitting coefficients. The variance of fatigue damage, normalized to expected damage squared ${}^{G}E[D(T)]^2$, defines the coefficient of variation (CoV):

$$ {}^{G}C_D = \sqrt{\frac{n + 2\sum_{l=1}^{n-1}(n-l)\ {}^{G}\rho_{d_0,d_l}}{n^2}\left(\frac{\Gamma(1+k)}{\Gamma^2\left(1+\frac{k}{2}\right)} - 1\right)} \tag{13} $$

5. Variance of damage: non-Gaussian case (new method)

5.1. Transformed model

The Low's method for a Gaussian process $X(t)$ can be extended to a non-Gaussian process $Z(t)$ provided that this is defined through a "transformed model" as $Z(t) = G(X(t))$. This "transformed model" is based on a time-independent non-linear transformation $G(-)$ that links the values of Gaussian and non-Gaussian processes at any time t. The Gaussian process $X(t) = g(Z(t))$ is retrieved by the inverse transformation $g(-) = G^{-1}(-)$.

Some authors (e.g. Winterstein, Ochi and Ahn, Lutes and Sarkani (2004)) provide the analytical expression of either the direct or the inverse transformation. Among them, only the Winterstein's model provides the expressions of both. This is particularly advantageous as it makes much easier to develop the following theoretical solution of the variance. Furthermore, the Winterstein's model is based on cubic Hermite polynomials that are capable to model non-Gaussian processes characterized by a relatively wide range of skewness, γ_3, and kurtosis, γ_4.

For a leptokurtic process ($\gamma_4 > 3$), the inverse transformation is (the time t variable is omitted for clarity) (Winterstein et al. (1994)):

$$ \begin{aligned} g(Z) &= \left[\sqrt{\xi^2(Z)+c} + \xi(Z)\right]^{\frac{1}{3}} - \left[\sqrt{\xi^2(Z)+c} - \xi(Z)\right]^{\frac{1}{3}} - a \\ \xi(Z) &= 1.5b\left(a + \frac{Z-\mu_Z}{\kappa\sigma_Z}\right) - a^3 \end{aligned} \tag{14} $$

in which μ_{Z} is the mean value and σ_{Z} the standard deviation of the non-Gaussian process, and $a = c_3/(3c_4)$, $b = 1/(3c_4)$, $c = (b - 1 - a^2)^3$. The scale factor $\kappa = (1 + 2c_3^2 + 6c_4^2)^{-1/2}$ assures that both the Gaussian and

non-Gaussian process has the same variance, $\sigma_X^2 = \sigma_Z^2$. The non-dimensional coefficients c_3 and c_4 take on slightly different expressions, depending on the version of the method. The earliest version (Winterstein (1985)) was a first-order model limited to small non-Gaussian degrees. The later version–considered in the following–included also a second-order term and gives the following expressions:

$$c_3 = \frac{\gamma_3}{6}\left[\frac{1 - 0.015|\gamma_3| + 0.3\gamma_3^2}{1 + 0.2(\gamma_4 - 3)}\right]; c_4 = c_{40}\left(1 - \frac{1.43\gamma_3^2}{\gamma_4 - 3}\right)^{1-0.1\gamma_4^{0.8}} \quad ; \quad c_{40} = \frac{[1 + 1.25(\gamma_4 - 3)]^{1/3} - 1}{10} \tag{15}$$

These coefficients hold for $0 < \gamma_3^2 < 2(\gamma_4 - 3)/3$ and $3 < \gamma_4 < 15$, which include most non-Gaussian cases. For a platykurtic process ($\gamma_4 < 3$), the inverse transformation is:

$$g(Z) = Z_0 - \tilde{c_3}(Z_0^2 - 1) - \tilde{c_4}(Z_0^3 - 3Z_0) \tag{16}$$

where $Z_0 = (Z - \mu_Z)/\sigma_Z$ is a standardized process; $\tilde{c_3} = \gamma_3/6$ and $\tilde{c_4} = (\gamma_4 - 3)/24$ are Hermite moments.

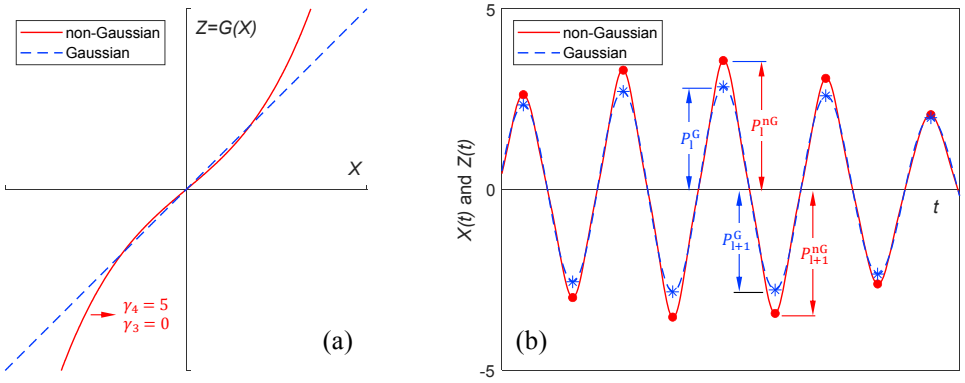

Fig. 1. (a) Non-linear transformation; (b) Gaussian and its corresponding transformed non-Gaussian process.

Fig. 1(a) depicts an example of non-linear transformation for $\gamma_3 = 0$ and $\gamma_4 = 5$. A Gaussian process and its corresponding transformed non-Gaussian are compared in Fig. 1(b). The peaks of both processes are marked to emphasize their relationship.

As a final comment, a shortcoming in the use of transformed models is that they tend to distort the power spectral density so that the power spectrum of the transformed process $Z(t)$ tends to be "whiter" (harmonics are added) than the spectrum of $X(t)$ (Smallwood (2005)). However, if the degree of non-linearity of $G(-)$ is not too high, the distortion is acceptable and both processes have similar spectral contents (Smallwood (2005)).

5.2. Variance for non-Gaussian process

The Low's model for the variance (see Sec. 4) relies on three known facts, namely that in a narrow-band process:

- the expected number of half-cycles in time interval T is proportional to the upcrossing rate: $E[n(T)] = {}^{G}\nu_0^+ 2T$;
- the time lag between two peaks P_i and P_{i+1} is $\tau = l/({}^{G}\nu_0^+ 2)$;
- the JPDF of two peaks is known in closed-form (Rice's distribution in Eq. (11)) if the process is Gaussian;

It should be noted that only the third point requires the Gaussian hypothesis for the process, whereas the other two are in fact very general and can be extended to a transformed non-Gaussian process. Indeed, the property of a "transformed model" of establishing a one-to-one relationship between instantaneous values in a Gaussian process

and its corresponding transformed non-Gaussian process has important consequences. It implies that both processes do have peaks, valleys and mean value crossings exactly at the same time instants, see Fig. 1(b). More precisely, if the Gaussian process crosses its mean value μ_{X} at time t_1, that is $X(t_1) = \mu_{\mathrm{X}}$, the non-Gaussian process will cross its mean value μ_{Z} also at t_1, that is $Z(t_1) = \mu_{\mathrm{Z}}$. Furthermore, if $X(t)$ has a peak $x_{\mathrm{p}}(t)$ or valley $x_{\mathrm{v}}(t)$ at instant t, the non-Gaussian process will have a corresponding peak or valley at the same instant, $z_{\mathrm{p}}(t) = G\big(x_{\mathrm{p}}(t)\big)$ and $z_{\mathrm{v}}(t) = G(x_{\mathrm{v}}(t))$. The same holds true also for the inverse relationship $x_{\mathrm{p}}(t) = g\big(z_{\mathrm{p}}(t)\big)$ and $x_{\mathrm{v}}(t) = g(z_{\mathrm{v}}(t))$. As a consequence of the previous property, both the Gaussian and non-Gaussian process have the same autocorrelation coefficient, that is $\rho_{\mathrm{X}}(l) = \rho_{\mathrm{Z}}(l)$.

Another, and perhaps more important, property is that the transformation–being monotonic–also preserves the relative position of peaks and valleys in both processes. This is to say, for example, that if $x_{\mathrm{p}}(t_1) > x_{\mathrm{p}}(t_2)$ at some instants t_1, t_2 in the Gaussian process, it will also be $z_{\mathrm{p}}(t_1) > z_{\mathrm{p}}(t_2)$ in the non-Gaussian process for the corresponding peaks transformed by $G(-)$ (of course, the same concepts applies to valleys as well). By using the notation adopted previously, if the Gaussian process has peaks ${}^{\mathrm{G}}P_l > {}^{\mathrm{G}}P_{\mathrm{l}+1}$ at time lag l, the non-Gaussian process will have peaks ${}^{\mathrm{nG}}P_{\mathrm{l}} > {}^{\mathrm{nG}}P_{\mathrm{l}+1}$ at the same time lag.

The previous arguments may be summarized by saying that a "transformed model" from Gaussian to non-Gaussian process preserves the number of mean value crossings and modifies (increases or decreases) the values of peaks and valleys (depending on γ_3, γ_4), keeping their relative positions unaltered. This property, in particular, guarantees that, in the non-Gaussian process, half-cycles are formed by peak/valley pairs transformed from the corresponding peak/valley pairs in the Gaussian process, and that non-Gaussian half-cycles have amplitudes smaller or larger (depending on γ_3, γ_4) than the corresponding amplitudes of Gaussian half-cycles.

In light of the previous arguments, the three conditions in the previous list may easily be adapted to the non-Gaussian case with no much effort. It is possible to say that in a narrow-band non-Gaussian process:

- the expected number of half-cycles in time interval T is $E[n(T)] = {}^{\mathrm{nG}}\nu_0^+ 2T$;
- the time lag between two peaks ${}^{\mathrm{nG}}P_{\mathrm{i}}$ and ${}^{\mathrm{nG}}P_{\mathrm{i+l}}$ is $\tau = l/\big({}^{\mathrm{nG}}\nu_0^+ 2\big)$;
- the JPDF of two peaks is obtained as a variable transformation of the Rice's joint distribution in Eq. (11);

The third point is now elaborated further. Let consider any two extremes z_{p} and z_{v} (peak and valley) in the non-Gaussian process. They are random variables with joint probability density function, say ${}^{\mathrm{nG}}\mathrm{f}_{\mathrm{P_0,P_l}}\big(z_{\mathrm{p}}, z_{\mathrm{v}}\big)$. Such extremes are transformed back to two corresponding extremes $x_{\mathrm{p}} = g\big(z_{\mathrm{p}}\big)$ and $x_{\mathrm{v}} = g(z_{\mathrm{v}})$ (peak and valley) in the Gaussian process through the inverse function $g(-)$. For the Gaussian extremes applies the joint Rice's distribution in Eq. (11). It is therefore straightforward to derive the joint distribution of the non-Gaussian extremes by the rule of transformed random variables (Lutes and Sarkani (2004)):

$$ {}^{nG}f_{P_0,P_l}\big(z_p, z_v\big) = {}^{G}f_{P_0,P_l}\big(x_p, x_v\big)\,\big|\,\mathbf{J}\big(x_p, x_v\big)\,\big|^{-1} \tag{17}$$

where symbol $|-|$ means "absolute value" and $\mathbf{J}$ is the Jacobian of the transformation $g(-)$, which turns out from the following 2×2 determinant:

$$\mathbf{J}\big(x_p, x_v\big) = \begin{vmatrix} \dfrac{\partial g(z_p)}{\partial z_p} & \dfrac{\partial g(z_p)}{\partial z_v} \\ \dfrac{\partial g(z_v)}{\partial z_p} & \dfrac{\partial g(z_v)}{\partial z_v} \end{vmatrix} \tag{18}$$

Note that the inverse transformation needs be applied to peak and valley variables separately. As a result, the Jacobian in Eq. (18) is, in fact, a diagonal matrix. Intuition indeed suggests, for example, that an infinitesimal change in the non-Gaussian peak ∂z_{p} cannot produce any variation in the corresponding valley ∂z_{v}, so that $\partial g\big(z_{\mathrm{p}}\big)/\partial z_{\mathrm{v}} = 0$. A similar reasoning applies to the other out-of-diagonal term to explain that $\partial g(z_{\mathrm{v}})/\partial z_{\mathrm{p}} = 0$.

By considering Rice's formula in Eq. (11), the general expression in Eq. (18) can be made more explicit as:

$$ {}^{nG}f_{P_0,P_l}(z_p,z_v) = \frac{g(z_p)g(z_v)}{1-\rho_Z^2} I_0\left(\frac{g(z_p)g(z_v)\rho_Z}{1-\rho_Z^2}\right) e^{\frac{g(z_p)^2+g(z_v)^2}{-2(1-\rho_Z^2)}} \left|\frac{\partial g(z_p)}{\partial z_p}\cdot\frac{\partial g(z_v)}{\partial z_v}\right|^{-1} \tag{19} $$

Although not written explicitly, the Bessel function $I_0(z_\mathrm{p}, z_\mathrm{v})$ in Eq. (19) is intended to be a function of z_p and z_v, and it is obtained by a simple change of variables in the corresponding function $I_0(x_\mathrm{p}, x_\mathrm{v})$ in Eq. (11), which is instead a function of x_p and x_v.

The expression in Eq. (19) represents the joint distribution of two peaks in the non-Gaussian process. The presence of a transformation of variables involving the non-linear function $g(z_\mathrm{p})$ makes the expression so complex that no closed-form solution is obtainable. A numerical approach is then adopted.

Eq. (19) depends on both γ_3 and γ_4 through function $g(z_\mathrm{p})$. It is also function of μ_Z, σ_Z^2 and ρ_Z. Obviously, in the limiting case $\gamma_3 = 0$ and $\gamma_4 = 3$ (Gaussian process), Eq. (19) converges to Rice's distribution in Eq. (11).

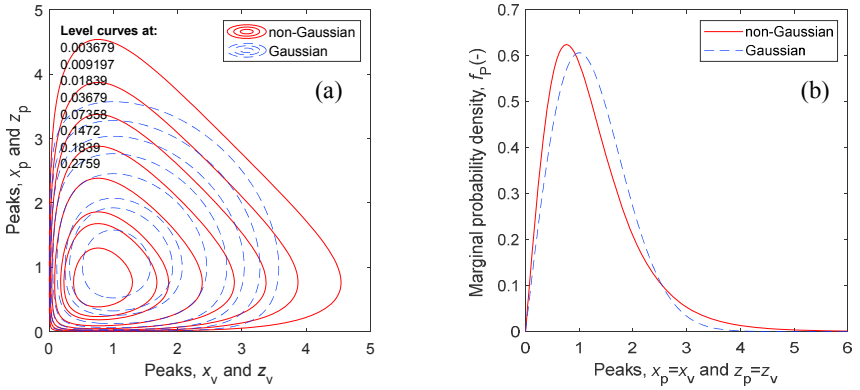

Fig. 2. (a) Peak-peak joint probability density function and (b) peak marginal distribution (solid line = Gaussian, dashed line = non-Gaussian).

Fig. 2(a) compares the Gaussian and non-Gaussian joint probability distributions (the latter obtained with $\mu_\mathrm{Z} = 0$, $\sigma_\mathrm{Z}^2 = 1$, $\rho_\mathrm{Z} = 0$, $\gamma_3 = 0$ and $\gamma_4 = 5$). The shift of probabilities is clear. In particular, if compared to the Gaussian case, the non-Gaussian distribution shows higher levels of probability towards larger peak values. The shift in probability is confirmed even more clearly by the comparison of the marginal probability density functions in Fig. 2(b).

The non-Gaussian peak-peak joint distribution obtained so far allows the damage correlation ${}^{\mathrm{nG}}E[d_0 d_\mathrm{l}]$ to be computed with no much effort by solving numerically the double integral in Eq. (10). The other damage terms in the variance expression of the non-Gaussian process are computed from the non-Gaussian peak probability distribution:

$$ {}^{nG}f_{P_0}(z_p) = {}^{G}f_{P_0}(x_p)\left|\frac{\partial g(z_p)}{\partial z_p}\right|^{-1} \tag{20} $$

which is transformed from the Rayleigh distribution of peaks, ${}^{\mathrm{G}}\mathrm{f}_{\mathrm{P}_0}(x_\mathrm{p})$, of the narrow-band Gaussian process. In Eq. (20), $x_\mathrm{p} = g(z_\mathrm{p})$ is the transformed variable corresponding to z_p.

In the same way as with Eq. (5), the expected damage ${}^{\mathrm{nG}}E[d_0]$ and ${}^{\mathrm{nG}}E[d_0^2]$ are nothing more than the moments of order k and $2k$, respectively, of the probability distribution ${}^{\mathrm{nG}}\mathrm{f}_{\mathrm{P}_0}(z_\mathrm{p})$. Making use of the expression in Eq. (20) and introducing the change of variable $g(z_\mathrm{p})$ into the Rayleigh distribution ${}^{\mathrm{G}}\mathrm{f}_{\mathrm{P}_0}(x_\mathrm{p})$, the two damage values can be written by this compact notation:

$$ {}^{nG}E\left[d_0^q\right] = \frac{1}{(2A)^q}\int_0^{\infty}\left[g(z_p)\right]^{q\cdot k}\,\frac{g(z_p)}{\sigma_Z^2}\,e^{-\frac{g(z_p)}{2\sigma_Z^2}}\left|\frac{\partial g(z_p)}{\partial z_p}\right|^{-1} dz_p \tag{21} $$

where the exponent q is 1 or 2. This expression is only a function of μ_Z, σ_Z^2, γ_3 and γ_4.

The variance of damage for the non-Gaussian process is finally obtained through Eq. (9), in which the terms ${}^{nG}E[d_0 d_l]$, ${}^{nG}E[d_0^2]$ and ${}^{nG}E[d_0]$ calculated so far for the non-Gaussian process need to be used:

$$ {}^{nG}\sigma_D^2 = n\left({}^{nG}E[d_0^2] - {}^{nG}E[d_0]^2\right) + 2\sum_{l=1}^{n-1}(n-l)\left({}^{nG}E[d_0 d_l] - {}^{nG}E[d_0]^2\right) \tag{22} $$

Accordingly, the coefficient of variation for the non-Gaussian process becomes:

$$ {}^{nG}C_D = \sqrt{\frac{n\left({}^{nG}E[d_0^2] - {}^{nG}E[d_0]^2\right) + 2\sum_{l=1}^{n-1}(n-l)\left({}^{nG}E[d_0 d_l] - {}^{nG}E[d_0]^2\right)}{n^2\,{}^{nG}E[d_0]^2}} \tag{23} $$

6. Numerical simulations

Monte Carlo simulations allow the correctness of the previous theoretical to be verified against time-domain results. Simulations considered a narrow-band rectangular power spectrum $S_X(f)$ centered at 10 Hz, with half spectral width 1 Hz and zero-order spectral moment $\lambda_0 = 1$, see Fig. 3(a). A total of $N = 2 \cdot 10^5$ random Gaussian time-histories $x_i(t)$, $i = 1,2,3,\ldots N$ were simulated from this PSD. Winterstein's model is then used to transform each $x_i(t)$ into a non-Gaussian time-history $z_i(t)$.

For every time-history, $x_i(t)$ and $z_i(t)$, the fatigue damage ${}^{G}D_i(T)$ and ${}^{nG}D_i(T)$ was calculated in time-domain by rainflow counting and Palmgren-Miner rule. Damage calculation assumed a S-N curve with $A = 1$ and several values of the inverse slope $k = 3, 5, 7$. The mean $\bar{D} = N^{-1}\sum_{i=1}^{N} D_i$, variance $\hat{\sigma}_D^2 = (N-1)^{-1}\sum_{i=1}^{N}(D_i - \bar{D})^2$ and coefficient of variation $\hat{C}_D = \hat{\sigma}_D/\bar{D}$ were estimated from the sample damage values in both Gaussian and non-Gaussian case. By contrast, the expected damage value was computed from the analytical solutions: the Gaussian expected damage ${}^{G}E[D(T)] = n\ {}^{G}E[d]$ from Eq. (6), the non-Gaussian expected damage ${}^{nG}E[D(T)] = n\ {}^{nG}E[d]$ by taking $q = 1$ in Eq. (21).

Fig. 3(b) shows the trend of mean and standard deviation of damage (normalized to the expected damage) as a function of the number of rainflow cycles, for both the Gaussian and non-Gaussian case (with $k = 3$, $\gamma_3 = 0$ and $\gamma_4 = 5$). It is apparent from the figure how the statistical scatter of damage decreases as the number of cycles in the loading increases. For any value of the number of cycles, the non-Gaussian damage always has a variance higher (about 100%) than that of the Gaussian damage. This difference confirms the importance of taking the non-Gaussian effect into account.

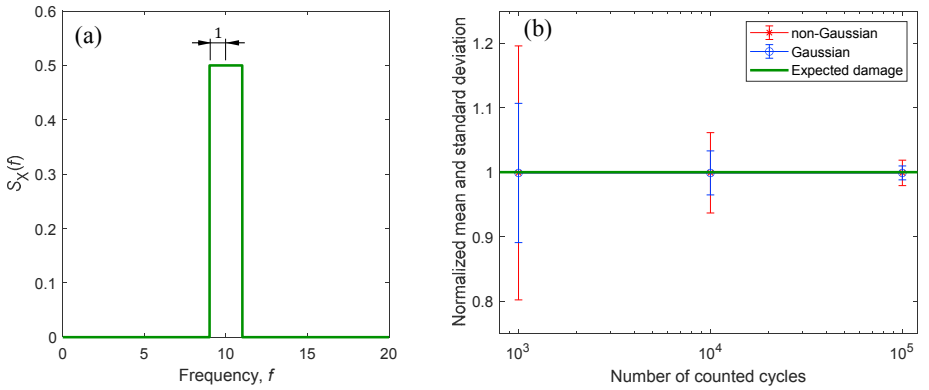

Fig. 3. (a) Narrow-band power spectrum; (b) trend of standard deviation (normalized to the expected damage) as a function of number of cycles

The trend in Fig. 3(b) is further clarified in Fig. 4(a), which shows the change of the coefficient of variation versus the number of counted cycles. Fig. 4(a) refers to an inverse slope $k = 3$. The two non-Gaussian cases have $\gamma_3 = 0.2$, $\gamma_4 = 2$ (platykurtic) and $\gamma_3 = 0.5$, $\gamma_4 = 8$ (leptokurtic). A perfect matching is observed between the proposed analytical approach (which coincides with Low's solution) and time-domain results in the Gaussian case. An equally perfect agreement between the proposed approach and time-domain results is obtained in non-Gaussian case either.

A small difference between time-domain and theoretical estimation may occur for very large kurtosis values (for example, $\gamma_4 > 6$), see Fig. 4(a). It comes from a numerical approximation that arises when calculating the joint probability distribution in the non-Gaussian domain (a non-Gaussian process indeed takes on much larger values than a Gaussian one, especially for very large γ_4). The results in Fig. 4(a) and (b) then confirm that not only is the proposed approach very accurate, but it also covers combinations of skewness and kurtosis over a wide range, $0 < \gamma_3^2 < 2(\gamma_4 - 3)/3$ and $1 < \gamma_4 < 15$ (i.e. limits of Winterstein's model).

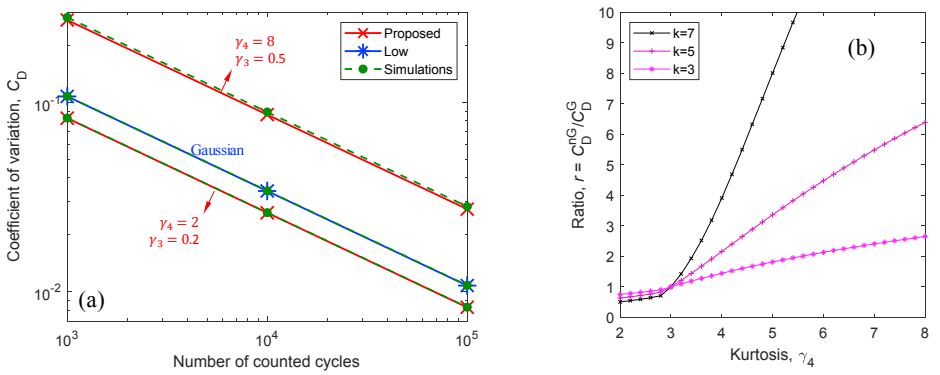

Fig. 4. Coefficient of variation: (a) analytical methods and time-domain simulations (b) Ratio $r = {}^{nG}C_D / {}^{G}C_D$.

Of more interest is the trend in Fig. 4(b). It displays the effect of load non-Gaussianity (kurtosis) and inverse slope on the coefficient of variation of fatigue damage, relative to a Gaussian load. The figure plots the ratio $r = {}^{nG}C_D / {}^{G}C_D$, where the numerator follows from Eq. (23) (non-Gaussian case) and the denominator from Eq. (13) (Gaussian case). In the region of platykurtic values ($\gamma_4 < 3$), the non-Gaussian loading is characterized by a lower statistical variation compared to Gaussian ($r < 1$). By contrast, in the region of leptokurtic values ($\gamma_4 > 3$) it always shows a larger variation ($r > 1$). It is also clearly apparent that, for a given kurtosis value, the ratio ${}^{nG}C_D / {}^{G}C_D$ markedly depends on the inverse slope k, for values of practical interest. For example, for $\gamma_4 = 5$, the increase is of

about 2 times for $k = 3$, while it can even arrive as large as 8 times for $k = 7$. This further confirms the importance of taking into account non-Gaussian effects in the evaluation of the variance of damage.

7. Conclusions

This work presented a theoretical model for assessing the variance of fatigue damage in stationary non-Gaussian random loadings with a narrow-band power spectrum. The model only requires that the power spectral density, skewness and kurtosis coefficients of the non-Gaussian loading are known. The model makes use of a time-independent non-linear transformation to link the Gaussian and non-Gaussian domains. This transformation is used to extend the range of validity of the existing Gaussian solution (Low's method) also to the non-Gaussian case.

Monte Carlo numerical simulations were presented to check the correctness of the proposed model and also to identify typical trends. A rectangular narrow-band PSD was used for simulating a large sample of random time-histories for which the variance of damage has been computed. It was observed that variance of damage for a non-Gaussian loading was larger (of about 100%) than the variance in a Gaussian loading. This result confirms how Gaussian models (which ignore non-Gaussian features) lead to unsafe estimates of the variance, especially for high values of kurtosis and inverse slope of the S-N curve. The use of the model here proposed is then recommended.

References

Benasciutti, D., Tovo, R., 2005. Spectral methods for lifetime prediction under wide-band stationary random processes. International Journal of Fatigue 27(8), 867–877.

Benasciutti, D., Tovo, R., 2018. Frequency-based analysis of random fatigue loads: Models, hypotheses, reality. Materialwissenschaft und Werkstofftechnik 49(3), 345–367.

Enzveiler Marques, J.M., Benasciutti, D., Tovo, R., 2019. Variance of fatigue damage in stationary random loadings: comparison between time- and frequency-domain results, 48th AIAS 2019 International Conference on Stress Analysis, Assisi, Italy.

Low, Y.M., 2012. Variance of the fatigue damage due to a Gaussian narrowband process. Structural Safety 34(1), 381–389.

Lutes, L.D., and Sarkani, S., 2004. Random vibrations: analysis of structural and mechanical systems, Elsevier Butterworth-Heinemann, Burlington, U.S.A.

Mark, W.D. 1961. The inherent variation in fatigue damage resulting from random vibration, Ph.D. thesis, M.I.T., Cambridge, U.S.A.

Rice, S.O., 1944. Mathematical analysis of random noise. Bell System Technology 23(3), 282–332.

Smallwood, D.O., 2005. Generating non-Gaussian vibration for testing purposes. Sound and Vibration 10, 18–24.

Winterstein, S.R., 1985. Non-normal responses and fatigue damage. Journal of Engineering Mechanics ASCE, 111(10), 1291-1295.

Winterstein, S.R., Ude, T.C., Kleiven, G., 1994. Springing and slow-drift responses: predicted extremes and fatigue vs. simulation, 7th International Conference on the Behaviour of Offshore Structures, M.I.T., Cambridge, U.S.A.